

# A BAYESIAN NON-LINEAR APPROACH FOR ELECTRICAL IMPEDANCE TOMOGRAPHY

Thierry MARTIN and Jérôme IDIER

Laboratoire des Signaux et Systèmes (CNRS-ESE-UPS)

Plateau de Moulon, 91192 Gif-sur-Yvette Cedex, France.

E-mail: martin@lss.supelec.fr, idier@lss.supelec.fr

## ABSTRACT

*Electrical Impedance Tomography* (EIT) of closed conductive media is an ill-posed inverse problem. As regards the corresponding direct problem, the choice of a *Finite Elements Method* preserves the non linear dependence of the observation set upon the conductivity distribution. In this paper, we show that the Bayesian approach presented in (1) for linear inverse imaging problems is also valid for a non linear problem such as EIT. Our contribution is based on an edge-preserving Markov model as prior for conductivity distribution. Reconstruction results obtained through the optimization of the posterior likelihood criterion yield significant resolution improvement compared to classical methods.

## 1 INTRODUCTION

*Electrical Impedance Tomography* (EIT) of closed conductive media with steady currents is a non-invasive imaging technique that aims at estimating the impedance distribution within a conductive body from electrical measurements on the surface. Applications can be found in medical imaging and non-destructive testing. Usually, thanks to surface electrodes, the experiment consists in injecting currents in the body and measuring the surface voltage distributions. In this paper, we deal with 2D reconstructions.

Contrary to many estimation problems studied so far (1), EIT is a *non linear* inverse imaging problem. Indeed, the current paths throughout the medium (and

thus the observations) highly depend on the conductivity distribution. The image-data relation, derived from Maxwell’s formulas, is ruled by a second order partial derivative equation. However, since this equation yields no analytical solution for arbitrary conductivity distribution, one has to approximate the direct problem. This kind of difficulty is widespread in inverse imaging problems. In Diffraction Tomography (2), the image-data relation, which is given by two coupled equations, is neither linear. Widespread approximations, introduced by neglecting the effects of diffraction, are Born and Rytov linearizations. In EIT, many authors (3, 4, 5) proposed linear approximations too. However, if the sought distribution is highly contrasted (which is often the case in EIT applications), linearized models are no longer valid.

Following (6), we opted for a *finite element method* (FEM) direct model, which preserves the non linear dependence of the observations upon the conductivity distribution. FEM convergence properties towards the true solution are well known, and this technique is frequently used in many problems involving partial differential equations (PDE), in such fields as electrostatics, solid or fluid mechanics... Besides, discretization of the 2D domain into elements reveals as also suited to a Bayesian approach of inversion, as shown in section II.

One of the major difficulties of EIT is its ill-posed character, which was ignored by the first reconstruction methods (3), based on simple backprojection techniques. As well as other methods developed so far, they provide estimators that are very sensitive to noise, for lack of regularization analysis. In section III, we show that the Bayesian approach presented in (1) is also a valid frame for ill-posed EIT.

The scope of our method is to reconstruct an image of *log-conductivity* elements, where each element enters the FEM triangle mesh system. We also consider a neighborhood system compatible with the mesh system. This allows the introduction of a Markov Random Field as a prior model for log-conductivity, which enables smooth reconstructions as well as detection of discontinuities. In section IV, we show that the *maximum a posteriori* estimate, which amounts to minimizing a regularized non convex criterion, yields high quality results.

## 2 F.E.M FOR THE OBSERVATION MODEL

Let us call  $\Omega$  the 2D domain and  $\bar{\Omega}$  its border. We respectively note  $I, V$  the current stream and voltage distributions on  $\Omega$  and  $\bar{I}, \bar{V}$  the same distributions restricted on  $\bar{\Omega}$ . Lastly, we call  $\sigma$  the conductivity distribution. On one hand, the direct problem consists in finding  $\bar{V}$  from  $\bar{I}$  and  $\sigma$ , while the inverse problem requires the determination of  $\sigma$  from  $\bar{I}$  and  $\bar{V}$ .

The observation model is described by the following PDE:

$$\operatorname{div}(\sigma \vec{\operatorname{grad}} V) = 0, \quad (1)$$

along with adequate additive current boundary conditions. In the general case, there exists no analytical solution (7) for this PDE. When linear approximations are too rough, one can resort to the following integral formulation of the problem, which is equivalent to Eq.(1):

$$\frac{1}{2} \int_{\Omega} \sigma |\vec{\operatorname{grad}} V|^2 d\mathbf{x} + \int_{\bar{\Omega}} V \frac{\partial \bar{I}}{\partial t} ds = 0. \quad (2)$$

This equation is better adapted to analysis than the PDE formulation. In particular, (8, 9) established that the exact observation model verifying Eq.(2) is well-posed. On the other hand, the corresponding inverse problem has a unique but unstable solution: the analytic inverse problem is ill-posed in the Hadamard sense.

According to the finite elements method (10, 11, 6, 12), the discretization of the problem amounts to divide the domain into, say  $P$  elements defining  $N$  nodes on  $\Omega$ , among which  $\bar{N}$  are on the border  $\bar{\Omega}$ . Thereafter, the discretized observation model reads:

$$\bar{\mathbf{v}} = \mathbf{P} \mathbf{A}(\boldsymbol{\sigma})^{-1} \mathbf{P}^{\top} \mathbf{D} \bar{\mathbf{i}}, \quad (3)$$

where  $\bar{\mathbf{v}}$  and  $\bar{\mathbf{i}}$  (of size  $\bar{N}$ , *i.e.* the number of border nodes) are discretized counterparts of  $\bar{V}$  and  $\bar{I}$ . The vector  $\boldsymbol{\sigma}$  contains the  $P$  elements of conductivity.  $\mathbf{A}$  is the  $(N - 1) \times (N - 1)$  « stiffness » matrix of the problem defined by:

$$a_{ij} = \sum_{n \in \epsilon(i) \cap \epsilon(j)} \sigma_n \theta(i, j, n), \quad (4)$$

where  $\epsilon(i)$  is the set of neighboring elements of node  $i$  and  $\theta(i, j, p)$  depends on the geometric features of the mesh on  $\Omega$ . The matrix  $\mathbf{A}$  is positive-definite and very sparse: in practice, more than 98% of its entries are null.  $\mathbf{P}$  is merely a  $\bar{N} \times (N - 1)$  border projection operator and  $\mathbf{D}$  is a difference operator defined by:

$$(\mathbf{D} \bar{\mathbf{i}})_n = \bar{i}_{n+1} - \bar{i}_{n-1} [\bar{N}], \quad (5)$$

*i.e.*, the current stream difference at the border, measured between the two neighbors of the  $n^{\text{th}}$  node. The matrix  $\mathbf{A}$  linearly depends on  $\boldsymbol{\sigma}$ , so the FEM image-data relation Eq.(3) is a non linear function of the conductivity distribution.

Actually, FEM discretization consists in approximation with functions: current stream and voltages are approximated by piecewise linear functions on each element, whose nodal values are respectively the components of  $\bar{\mathbf{i}}$  et  $\bar{\mathbf{v}}$  while conductivity is approximated through piecewise constant functions whose element values belong to  $\boldsymbol{\sigma}$ . Let us mention that FEM approximation is practically much finer

than linear since this method has a  $O(r^2)$  convergence rate where  $r$  is the widest element diameter (10) while the computational cost, essentially lying in the inversion of the matrix  $\mathbf{A}(\boldsymbol{\sigma})$ , is highly reduced thanks to sparse matrix inversion algorithms.

### 3 A BAYESIAN INVERSE APPROACH

#### 3.1 Ill-posedness of the algebraic inverse problem

The condition number of  $\mathbf{A}(\boldsymbol{\sigma})$  does not exceed  $10^4$ , so Eq.(3) provides a numerically stable solution to the direct problem. The knowledge of  $\bar{\mathbf{i}}$  ( $\bar{N} \times 1$ ) and  $\boldsymbol{\sigma}$  ( $P \times 1$ ) allows to compute  $\bar{\mathbf{v}}$  ( $\bar{N} \times 1$ ). On the other hand, there exists no inverse way to get  $\boldsymbol{\sigma}$  from the observation. First of all, since we have  $\bar{N} < N < P$ , the number of data  $\bar{N}$  is lower than the number of unknowns  $P$ . In practice,  $K$  independent observation sets are gathered, with  $K > P/\bar{N}$ , so that classical back-projection techniques are implementable (3, 12). Such methods aim at minimizing the quadratic distance between the observations and the FEM direct simulation. Yet, these methods provide no acceptable results. This is not surprising since, we guess, a small change on inner conductivity has very few influence on the observation on the border. On the other hand, given the ill-posed character of the inverse problem, the backprojected image may rather depict amplified noise rather than true conductivity values.

#### 3.2 Bayesian regularization

In 1991, Hua *et al.* (6) proposed to add a quadratic penalty term to the usual criterion. Its regularizing effect is well-known and provides robust conductivity maps, but at the expense of poor resolution. Here we propose to introduce another kind of penalty term, corresponding to a non-Gaussian Markov prior probability from the Bayesian point of view. On the other hand, following Barber and Brown (4), the use of the log-conductivity  $\gamma = \log(\sigma)$  is preferred. Unlike  $\sigma$ , it needs not be constrained positive. Besides, the mapping  $\bar{\mathbf{v}}(\gamma)$  looks closer to linearity than  $\bar{\mathbf{v}}(\boldsymbol{\sigma})$ . Both features make the penalized criterion easier to optimize with respect to  $\gamma$ . It is defined as the Bayesian posterior likelihood:

$$p(\gamma | \bar{\mathbf{v}}^k; \bar{\mathbf{i}}^k) \propto p(\bar{\mathbf{v}}^k | \gamma; \bar{\mathbf{i}}^k) p(\gamma). \quad (6)$$

If we consider a centered white Gaussian noise  $\bar{\mathbf{n}}^k$  of variance  $\lambda^2$ , for the  $K$  direct observation models  $k = 1, \dots, K$ :

$$\bar{\mathbf{v}}^k = \mathbf{P} \mathbf{A}(\boldsymbol{\sigma})^{-1} \mathbf{P}^\top \mathbf{D} \bar{\mathbf{i}}^k + \bar{\mathbf{n}}^k, \quad (7)$$

we get the likelihood:

$$p(\bar{\mathbf{v}}^k | \boldsymbol{\gamma}; \bar{\mathbf{t}}^k) \propto \exp - \frac{1}{2\lambda^2} \sum_{k=1}^K \|\bar{\mathbf{v}}^k - \mathbf{P}[\mathbf{A}(e^{\boldsymbol{\gamma}})]^{-1} \mathbf{P}^\top \mathbf{D} \bar{\mathbf{t}}^k\|^2. \quad (8)$$

In EIT applications, especially in medical imaging, conductivity distributions are often homogeneous areas, separated by discontinuities. Therefore, we suggest to use the 2D mesh structure itself to introduce a Markov Random Field (MRF) as prior. Let  $v(p)$  be the set of spatial neighbors of the  $p^{\text{th}}$  element ( $v(p)$  contains three elements at most), and let us introduce the  $\mathcal{C}^1$  convex Huber penalty function defined by:

$$h_T(t) := \begin{cases} t^2 & \text{if } |t| < T, \\ 2T|t| - T^2 & \text{otherwise} \end{cases}$$

and the prior probability  $p(\boldsymbol{\gamma}) = \exp -\Phi_T(\boldsymbol{\gamma})$ , with

$$\Phi_T(\boldsymbol{\gamma}) = \frac{1}{2} \sum_{p=1}^P \sum_{q \in v(p)} h_T(\gamma_p - \gamma_q). \quad (9)$$

$h_T(\gamma_p - \gamma_q)$  favours local smoothness thanks to its near-to-zero parabolic zone, but it also allows discontinuities between pixels thanks to the linear parts (13). As a result, computing the *maximum a posteriori* amounts to minimizing the following criterion:

$$J(\boldsymbol{\gamma}) = \sum_{k=1}^K \|\bar{\mathbf{v}}^k - \mathbf{P}[\mathbf{A}(e^{\boldsymbol{\gamma}})]^{-1} \mathbf{P}^\top \mathbf{D} \bar{\mathbf{t}}^k\|^2 + 2\lambda^2 \Phi_T(\boldsymbol{\gamma}). \quad (10)$$

This criterion is the sum of a non convex likelihood term and a prior convex term. The latter reduces the global non convexity of  $J(\boldsymbol{\gamma})$ , so it favours its minimization, even toward a local minimum. Hua *et al.*, who have a white Gaussian regularization term with respect to  $\boldsymbol{\sigma}$ , use a Newton-Raphson (14) method to minimize their criterion. This second order algorithm is computationally heavy because it requires Hessian approximation, and looks inadequate because the criterion has not a parabolic shape. We preferred a first order descent method: the conjugate gradient algorithm (14), which proves simpler and faster.

#### 4 IMPLEMENTATION AND RESULTS

For the purpose of illustration, let us estimate the conductivity of a circular objet. Its conductivity consists of a homogeneous background of  $10 \text{ S.m}^{-1}$ , with two strongly contrasted areas of  $100 \text{ S.m}^{-1}$  and  $1000 \text{ S.m}^{-1}$  (cf. Fig.1). The domain is discretized into  $\bar{N} = 32$  border points,  $N = 145$  nodes and  $P = 256$  elements. We assume that  $256/32 = 8$  different current distributions are available, which

are successive rotations of the same sine period. This function is proven (15) to generate straight current lines when the conductivity distribution is uniform.

Since the problem is very ill-posed, most of the authors considered either free of noise examples (3), or otherwise very weakly degraded. Hua *et al.* worked on real objects and estimated the observation uncertainty measure to 1/2000 (66 dB). Besides, they used the measurable uniform background conductivity of the original distribution as the starting point of their minimization algorithm. We initialize our gradient minimization algorithm in the same way, and we assume a 1000 (60 dB) signal-to-noise ratio.

The results are obtained with three different reconstruction methods: the first works without regularization, the second with quadratic (Markov-Gauss) regularization and the third is the proposed method. It takes about one hour to perform the minimization with *Matlab 4.2* software on a *HP 712* workstation. Parameter  $\lambda$  for the quadratic term and  $(\lambda, T)$  for the Huber function were chosen empirically to get the best qualitative reconstruction results.

In order to compare the quality of the reconstructions  $\hat{\gamma}$ , we measure the  $\mathcal{L}^1$  distance to the original, which is known to be in good agreement with visual appreciation. More precisely, we use the following discrepancy measure:

$$\delta_1(\gamma, \hat{\gamma}) = \frac{\|\gamma - \hat{\gamma}\|_1}{\|\gamma\|_1}. \quad (11)$$

Method	$\lambda$	$T$	$\delta_1(\gamma, \hat{\gamma})$
No regul.	$\lambda = 0$	$T = \infty$	1.128
Gaussian	$\lambda = 8 \cdot 10^{-4}$	$T = \infty$	0.948
Huber	$\lambda = 2.5 \cdot 10^{-3}$	$T = 0.03$	0.519

The table above, as well as reconstructions (cf. Figs.2, 3 and 4), show that regularization is not only useful but necessary, and that the convex Huber function is relevant for the reconstruction of discontinuities.

## 5 CONCLUSION

In this paper, we propose a new EIT reconstruction algorithm based on a Bayesian formulation. EIT is a difficult non linear ill-posed inverse problem. We show how to combine a FEM direct solver and a non-Gaussian Markov field as a prior model on elements of log-conductivity.

Further improvements might be expected from relaxation techniques (16, 17), in order to avoid local minima. We also study the possibility of implementing mesh refinements as a multiscale tool.

## ACKNOWLEDGMENT

The first author cordially thanks Andrew Adler, from the *Institut de Génie Biomédical de Montréal*, who provided the FEM code used in this paper.

## REFERENCES

- (1) G. Demoment, “Image reconstruction and restoration : Overview of common estimation structure and problems”, *IEEE ASSP*, vol. 37, no. 12, pp. 2024–2036, Dec. 1989.
- (2) H. Carfantan and A. Mohammad-Djafari, “A Bayesian approach for nonlinear inverse scattering tomographic imaging”, in *Proceedings of IEEE ICASSP*, Detroit, U.S.A., May 1995, vol. IV, pp. 2311–2314.
- (3) M. Tasto and H. Schomberg, “Object reconstruction from projections and some non-linear extensions”, *Pattern Recognition and Signal Processing (ed. C. H. Chen)*, pp. 485–503, 1978.
- (4) D. Barber and B. Brown, “Recent developments in applied potential tomography”, *APT Information Processing in Medical Imaging*, pp. 106–121, 1986.
- (5) C. Cohen-Bacrie, “Régularisation du problème inverse de tomographie d’impédance électrique”, Master’s thesis, École polytechnique de Montréal, Dec. 1994.
- (6) P. Hua, E. Woo, J. Webster, and W. Tompkins, “Iterative reconstruction methods using regularization and optimal current patterns in electrical impedance tomography.”, *IEEE trans. Med. Imag.*, pp. 621–628, dec 1991.
- (7) M. Renardy and R. Rogers, *An Introduction to Partial Differential Equations*, Springer-Verlag, 1993.
- (8) J. Sylvester and G. Uhlmann, “A global uniqueness theorem for an inverse boundary value problem”, *Ann. Math.*, vol. 125, pp. 153–169, 1987.
- (9) G. Alessandrini, “Stable determination of conductivity by boundary measurements”, *Applicable Analysis*, vol. 27, pp. 153–172, 1988.
- (10) A. J. Davies, *The Finite Element Method: A First Approach*, Oxford Applied Mathematics and Computing Science Series, 1980.
- (11) J. Webster, *Electrical Impedance Tomography*, Adam Hilger, IOP Publishing Ltd, 1990.
- (12) R. V. Kohn and A. McKenney, “Numerical implementation of a variational method for electrical impedance tomography”, *Inverse Problems*, pp. 389–414, 1990.
- (13) P. Huber, *Robust Statistics*, New York: John Wiley & Sons, 1981.
- (14) B. Polyak, *Introduction to optimization*, Optimization Software, Inc., 1987.
- (15) D. Gisser, D. Isaacson, and J. Newell, “Current topics in impedance imaging”, *Clin. Phys. Physiol. Meas.*, vol. 8 Suppl. A, pp. 39–46, 1987.
- (16) A. Blake and A. Zisserman, *Visual Reconstruction*, Cambridge, MA: MIT Press, 1987.
- (17) M. Nikolova, A. Mohammad-Djafari, and J. Idier, “Inversion of large-support ill-conditioned linear operators using a Markov model with a line process”, in *Proceedings of IEEE ICASSP*, Adelaide, Australia, 1994, vol. V, pp. 357–360.

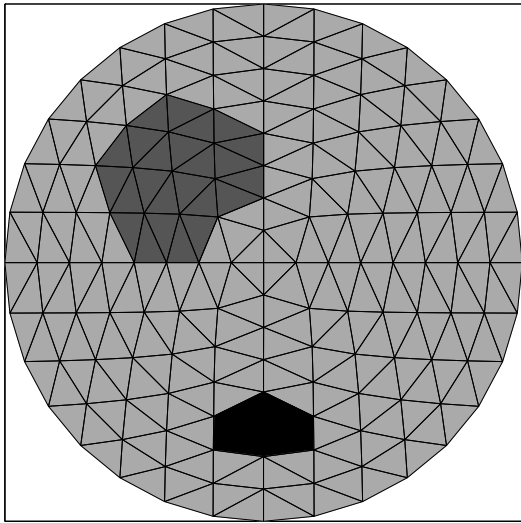


FIG. 1 - *The original conductivity distribution.*

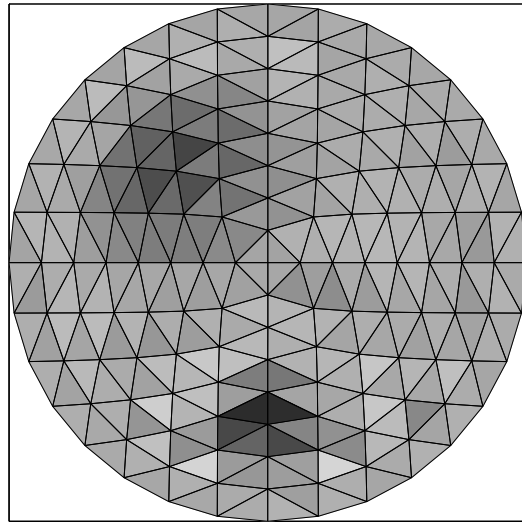


FIG. 2 - *Reconstruction without regularization.*

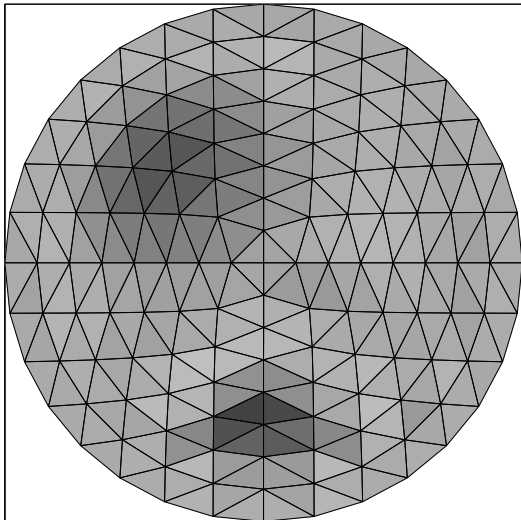


FIG. 3 - *Reconstruction with Gauss-Markov prior.*

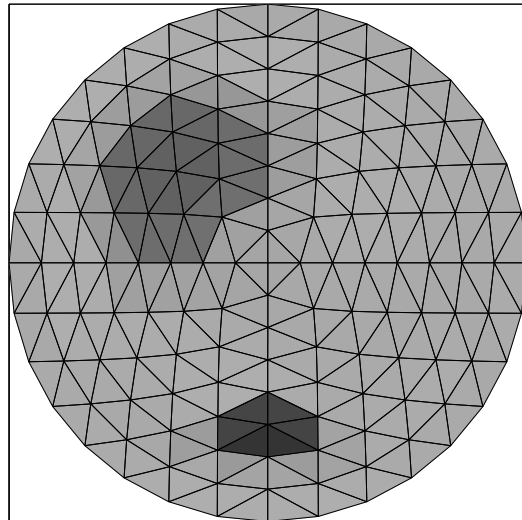


FIG. 4 - *Reconstruction with Huber prior.*



FIG. 5 - *Scale used for the conductivity distribution.*